

TURBULENT FLOWSTRUCTURE COMPUTATION INSIDE A PUMP-PAT USING AN INDUSTRIAL BENCHMARK TEST CASE

Fábio J. Silva[†], José C. Páscoa^{†1}, João S. Pinheiro^{††} and Daniel J. Martins^{††}

[†]University of Beira Interior,
Electromechanical Engineering Department
R. Mq.s DÁvila e Bolama, 6201-001 Covilhã, Portugal
e-mail: fabio_jas@hotmail.com, pascoa@ubi.pt

^{††}EFAFLU Bombas e Ventiladores S.A.
R. S. Brás, 269, Apartado 23, 4494-909 Póvoa do Varzim, Portugal
e-mail: spinheiro@efafllu.pt, dmartins@efafllu.pt

Key words: Centrifugal Pump, Impeller, Turbulence Modeling, Spalart-Allmaras, PAT

Abstract. *The complexity of any study on the flow in a centrifugal impeller is obvious and has stirred the research work over the last decades. Many studies have been carried out, but even nowadays some flow occurrences are still under study and far from being fully understood. The paper shows results for the numerical simulation of the three-dimensional fluid flow inside a centrifugal pump. A turbulent RANS computation is performed using Spalart-Allmaras turbulence model. The simulation has been made with a frozen rotor approach in order to take into account the impeller-volute interaction. Using this approach we are able to simulate the flow in the blade passage, in front of the tongue, and the overall turbomachine flow field. Results are also given for five different flow rates. A detailed analysis on the flow structure inside the pump is performed for design and two off-design conditions. For these numerical computations we perform a comprehensive examination of the loss distribution using the computed values for stagnation pressure loss. Evidence of recirculating regions is detected by computing the streamlines on a characteristic plane. An unconventional application of the pump is computed for the Pump-As-Turbine (PAT). Data is presented for the changes in the flow structure, by comparison between the pump running in direct (pump) and in reverse (turbine) modes. The data thus obtained allow an analysis of the main phenomena occurring in these two distinctive working modes. With the presented computations we were able to define the fidelity of a full CFD pump computation, by using an industrial pump as a benchmark test case.*

¹Corresponding Author.

1 INTRODUCTION

The flow inside a turbomachine is highly complex due mainly to the 3D flow structures involving turbulence, secondary flows, cavitation and unsteadiness. Traditional design approaches for centrifugal pumps were based on empirical correlations, a combination of model testing and engineering inspired experience. This has conducted, over the years, to the design of centrifugal pumps with remarkable performance trends see, e. g., Efaflu - Bombas e Ventiladores S.A. industrial pump series¹. However, present day design practices demand for a detailed understanding of the internal flow for design, and off-design, operating conditions. In this regard Computational Fluid Dynamics (CFD) started to play a key role for the prediction of the flow through pumps, and turbines, having successfully contributed to the enhancement of their design².

A growing availability of computer power, and a progress in accuracy of numerical methods, brought turbomachinery CFD methods from pure research work, into the competitive industrial markets^{3, 4}. In late 90's numerical codes started to evolve, from a pure inviscid physical model assumption, into realistic viscous turbulent models. Due to the high computer power involved these later models were only applied to study 2D, or quasi-3D, simplified isolated components of the pumps⁵, e. g., impeller, volute and guide vanes. In recent years the ability to perform full 3D computations for the global pump geometry become feasible⁶. Yet, we must bear in mind that, for a useful and correct interpretation of the CFD computed flow fields; the designer must have a deep knowledge on the physical basis underlying the flow inside turbomachinery. For features of detail, such as the wear-ring seals, a coupled analytical–numerical approach is used⁷. Moreover, due to the empirical nature of turbulence models applied in these computations, it is of paramount importance to compare the computed results with experimental testing in order to achieve good pump designs⁸.

With the aim of using CFD to model pump flows we usually apply three different approaches; frozen-rotor, mixing-plane, and pure unsteady computation. The most demanding, in what regards to computer power, is the unsteady flow computation approach. In the frozen-rotor approach we perform a quasi-steady computation of the flow. In this approach the impeller grid is frozen in time, which makes it most accurate to compute axial flow pumps. The mixing-plane approach performs an averaging of the flux variables between the planes defining the stator and rotor fluids, this allows to take into account unsteady effects in an approximate way, both for centrifugal and axial impellers. Actually, and for axial impellers, it allows us to model the rotor as comprising only one blade passage. This can substantially reduce the grid node count, and therefore allows a faster computation. In the unsteady approach the rotor and stator meshes are allowed to slide, in the continuity faces, between static and moving fluid. For this case a full converged solution must be obtained in each time-step, and the time-step must be sufficiently small to achieve a good resolution of the unsteady frequencies.

To set-up a full computation of a centrifugal pump we usually resort to a frozen-rotor

or to an unsteady computation, as for this class of problems the mixing plane assumption results in convergence problems. This is due to the small gap between rotor and stator in the pump tongue zone. Yet, it is advisable to use the mixing plane model in cases where the gap is enough to sustain a good convergence of the numerical code, as is the case for high volute-rotor ratios. For the present computations we have applied a frozen-rotor approach due to the existence of a small gap between rotor and tongue.

A key factor that undermines the expansion of CFD pump design, namely for routine industrial computations, is related to turbulence modeling. Computation of turbulent flow inside hydraulic pumps can, at present day, only be routinely performed by solving the RANS equations. By time averaging the equations we must define a model to compute the Reynolds stresses. Instead of solving for the Reynolds stresses the usual practice is to implement an eddy viscosity model. In order to compute the eddy viscosity diverse turbulence models have been developed and applied, namely $k - \epsilon$, $k - \omega$ and Spalart-Allmaras among others. All these models are available in the Fluent commercial code. In our present work we have applied $k - \epsilon$ and Spalart-Allmaras turbulence models, however we will only present results for the Spalart-Allmaras. This model resulted in more accurate prediction of pump flow when compared with results obtained from experimental testing. Some of the methods can not be used to integrate the governing equations up to the wall. These are usually referred as high-Re turbulence models, as is the case of $k - \epsilon$. Conversely Spalart-Allmaras is a low-Re turbulence closure and it can be used to compute wall bounded flows, but this implies that the near-wall mesh must have a high node density. This increased computing burden would turn out the full pump computation almost impossible, except on supercomputers, thus bearing an unattainable cost for daily pump design practice. To overcome this problem we have applied standard wall functions, in order to achieve the computation with lower computational costs. Albeit this, several pump meshes need to be generated in order to achieve an y^+ between 30 and 300, in order to ensure that we are under the range of applicability of wall functions.

In the present paper a high performance centrifugal pump, from Efaflu - Bombas e Ventiladores S.A.¹, will be analyzed as an industrial benchmark test case. Many of the true 3D computations usually presented in the open literature are for simplified geometries. A vast majority comprises rotors with non-curved blades and, indeed, authors also clean up some of the geometric details. In our approach all the pump details will be modeled, thus bearing a considerable challenge on mesh generation and on an adequate definition of the interface planes. In Section 2 we describe the test case including their experimental results; in Section 3 a complete description of the numerical results obtained for the design and two off-design points is also presented, furthermore results are also presented for the pump working in reverse turbine mode. Finally, in Section 4, conclusions are drawn from a detailed analysis of the results.

2 CENTRIFUGAL PUMP BENCHMARK TEST CASE

Herein we will describe the pump geometry and the numerical model used to compute the flow. In order to fully describe the test case we present details of the experimental pump testing facility at Efaflu - Bombas e Ventiladores S. A..

2.1 Geometry and grid for the NNJ 125-250 centrifugal pump

An accurate definition of the geometry is of primary importance to achieve a precise numerical modeling of the pump. In the present work this was certified by the creation of the mesh using a 3D CAD file from the manufacturer.

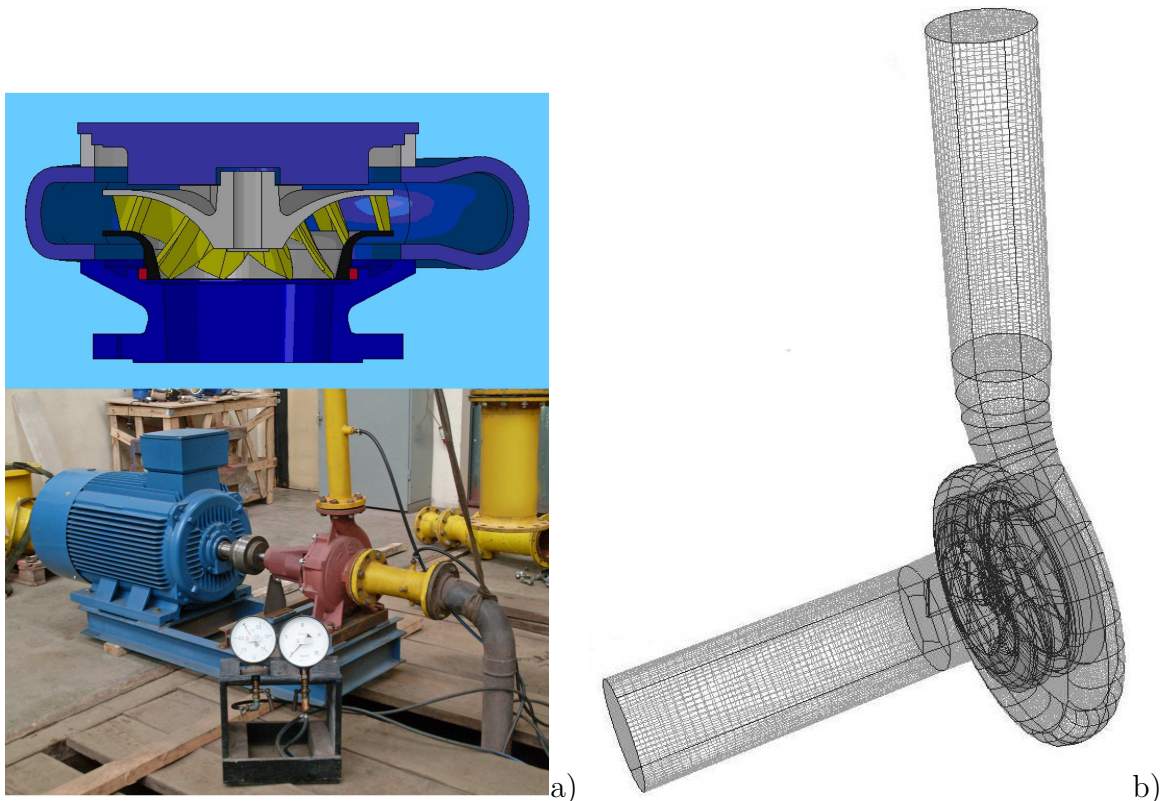


Figure 1: NNJ 125-250 130 kW centrifugal pump: a) Sectional view of the pump and partial view of the experimental facility, typical measurements are for flowrate and manometric pressure at pump inlet and outlet. b) The corresponding computational mesh used to perform the computations with 2 134 777 volumes.

The pump to be modeled is from NNJ series, it is an extremely complex geometry as can be seen in Fig.1-a), who depicts a sectional view of the pump. Flow enters from the image bottom and evolves in the centrifugal rotor exiting in radial direction on the casing volute. Figure 1-a) also presents an overall view of the experimental testing facility at Efaflu - Bombas e Ventiladores S. A. A typical normalized procedure is conducted in order

Table 1: Definition of the several geometrical grid blocks, imposed boundary conditions and numerical model.

Parameter	Numerical grid
Domain of simulation	Block A + Block B + Block C (impeller – 8 blade passages) + Block D + Block E + Block F + Block G + Block H + Block I + Block J (volute casing) + Block K + Block L
Extended inlet duct grid	Unstructured 135 129 cells (tet + pyr)
Extended outlet duct grid	Unstructured 87 461 cells (tet + pyr)
Impeller grid	Unstructured 881 138 cells (tet + pyr)
Volute casing grid	Unstructured 407 017 cells (tet + pyr)
Block D	Structured 9 555 cells
Boundary conditions and numerical methods	
Inlet	Total pressure = 0 Pa
Outlet	Gauge pressure = 735 671.5 Pa
Interface impeller/volute	Frozen Rotor
Turbulence model	Spalart-Allmaras
Spatial discretization	Second order

to obtain the experimental characteristic curves for the pump. In Fig.1-b) we can see the grid generated to perform the numerical computations, this comprises 2 134 777 volumes.

The shrouded rotor, with a nominal diameter of 265 mm, is composed by 8 blades. The complexity of the geometry is further increased by 6 additional vanes facing the rotor from backwards. These were also modeled and can be seen in Fig.2-c). The suction side includes a guiding vane visible in Fig.2-a), thus reducing inlet swirl. The inlet suction pipe section has a diameter of 148.50 mm that becomes 125 mm at the pressure section. More details on the geometry and pump data are available from ref.1, see also manufacturer catalogues at <http://www.efafllu.pt>.

In order to obtain a good mesh quality we have performed detailed aspect-ratio and equi-angle adjustments on mesh domain node distribution. Finally, the grid is composed by 12 geometrical blocks, see Tab.1. Some of the most important blocks are visible in Fig.2. For each of the blocks we construct interfaces that allow the transfer of cinematic variables between the bordering fluid blocks. Besides the geometrical blocks we also define two fluid blocks, these comprise the stationary and rotating fluid. A rotating fluid block is defined in the rotor and a second rotating fluid block is also defined for the rotor backward vanes. The remaining fluid is considered in a stationary reference frame.

2.2 Numerical model

The numerical model is implemented using FLUENT 6.3 commercial code. We model the flow by computing the Reynolds Averaged Navier-Stokes equations for 3D, including the centrifugal force effects in rotor. We consider incompressible flow and march to steady state using a pseudo-unsteady approach. Currently we have performed computations

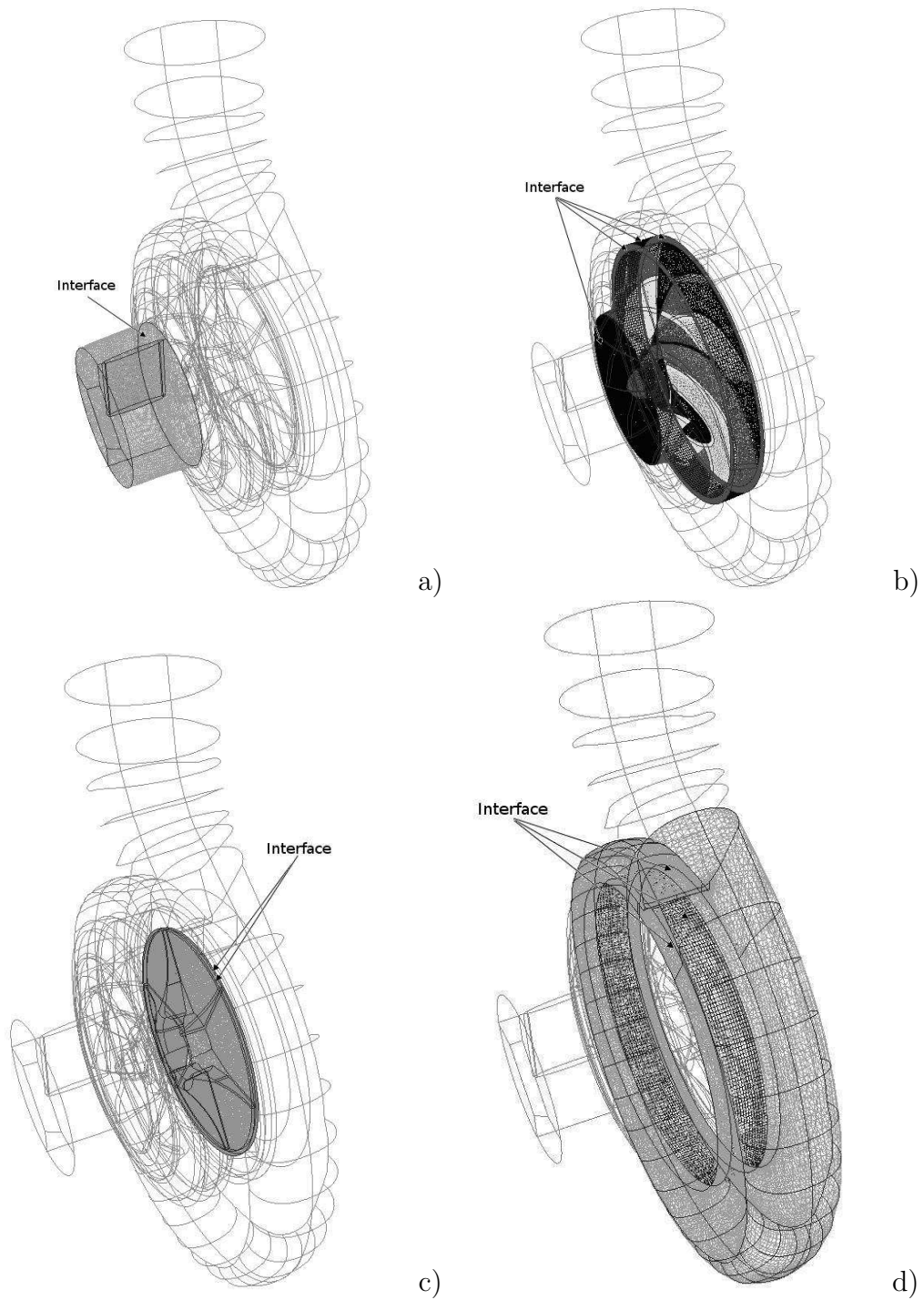


Figure 2: Details of the grid block assembly for the centrifugal pump: a) Inlet guide vane block between suction block and rotor block. b) Rotor block comprising a pure unstructured grid due to the geometry complexity. c) Moving fluid block associated to the back-rotor vanes. d) Volute casing block defined in a stationary reference frame.

using the $k - \epsilon$ and Spalart-Allmaras turbulence models, but we will only present the best available results using Spalart-Allmaras. Albeit this is a low-Re turbulence model we apply standard wall functions in order to reduce computing load. Second-order precision in space is selected to obtain the final results, although for increased convergence we started computations using a first-order discretization. A finite-volume discretization using PISO algorithm for pressure-velocity coupling was used to obtain the solution. In order to achieve convergence, in particular due to the high complexity of the mesh, a coupled solution method for the system of equations was retained. All the results presented in this work have been obtained using a frozen-rotor approach, mainly because the convergence of mixing-plane results was impossible to obtain, as expected, in view of the high volute-rotor radius ratio.

In the current literature different type of boundary conditions are considered for the computation of pump flows^{9, 10}. Most of the present results available in the literature apply a mixed type condition, using static pressure at outlet and mass flow at inlet. It is usually referred that this is the most robust condition to apply in order to achieve convergence. However, it is this author's opinion that a more natural condition could be applied, and convergence attained, if an adequate definition of the grid is performed. This turn out to be the case of the results presented in the present work, we have thus imposed a stagnation pressure at inlet and static pressure at outlet. The inlet stagnation pressure can be referred to pressure head $\Delta P = P_2 - P_1$. The moving reference frame was applied to the rotating fluid; all the results were obtained for a nominal pump rotation of 2900 rpm.

3 RESULTS FOR THE FLOW ON THE CENTRIFUGAL PUMP

This section will describe the results obtained for the centrifugal pump under study. Results will provide a description of the flow field for design and off-design conditions.

3.1 Analysis of the flow on the pump

Herein we present results for the analysis of the flow in the centrifugal pump for design and off-design conditions. Figure 3 presents a comparison between experimental and numerical results at the design point (around 122.07 l/s) and also for values ranging from 99.42 to 130.20 liters per second. The experimental results were obtained in the experimental facilities depicted in Fig1-a). Experimental results present a relative error below 2%. The numerical results present values, consistently, below the experimental curve. This behavior, around 5%, is to be expected as we are computing the flow using a frozen rotor model. These results would present diverse values as we froze the rotor in different rotating positions. Actually, we have already performed preliminary computations that suggest that the values will increase for other relative rotating positions between the blade and impeller.

Figure 4 gives an insight on how the flow structure inside the pump is changing for

off-design conditions. In this figure we can check how the static pressure is evolving in the volute casing. A more detailed analysis can be performed by looking at the streamline pattern for the two off-design points, see Fig.5. It is interesting to observe the occurrence of a recirculating bubble for the case of $1.07Q_n$. This is not observed in the computations obtained for part load.

Numerical			Experimental	
Q [l/s]	ΔP [Pa]	H [m]	ΔP [Pa]	H [m]
99.42	817 250.7	83.3	873 090.0	89.0
114.70	782 738.4	79.8	825 000.0	84.1
122.07	760 636.7	77.5	810 000.0	82.7
128.06	738 152.6	75.2	787 500.0	80.3
130.20	729 105.4	74.3	781 250.0	79.6

Figure 3: Comparison between the experimental results and the results obtained with the numerical model. Static pressure values are presented for range three working conditions.

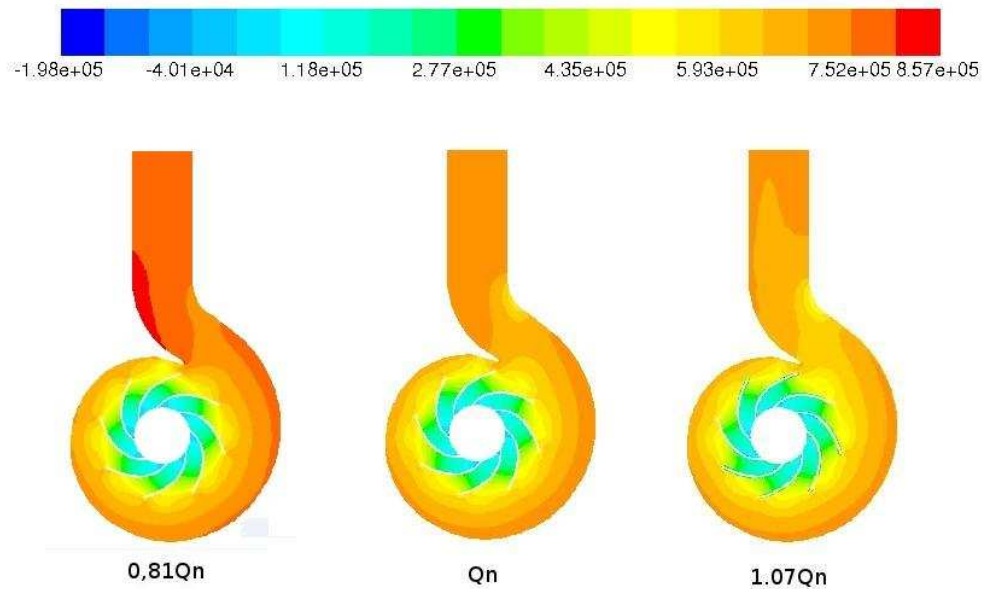
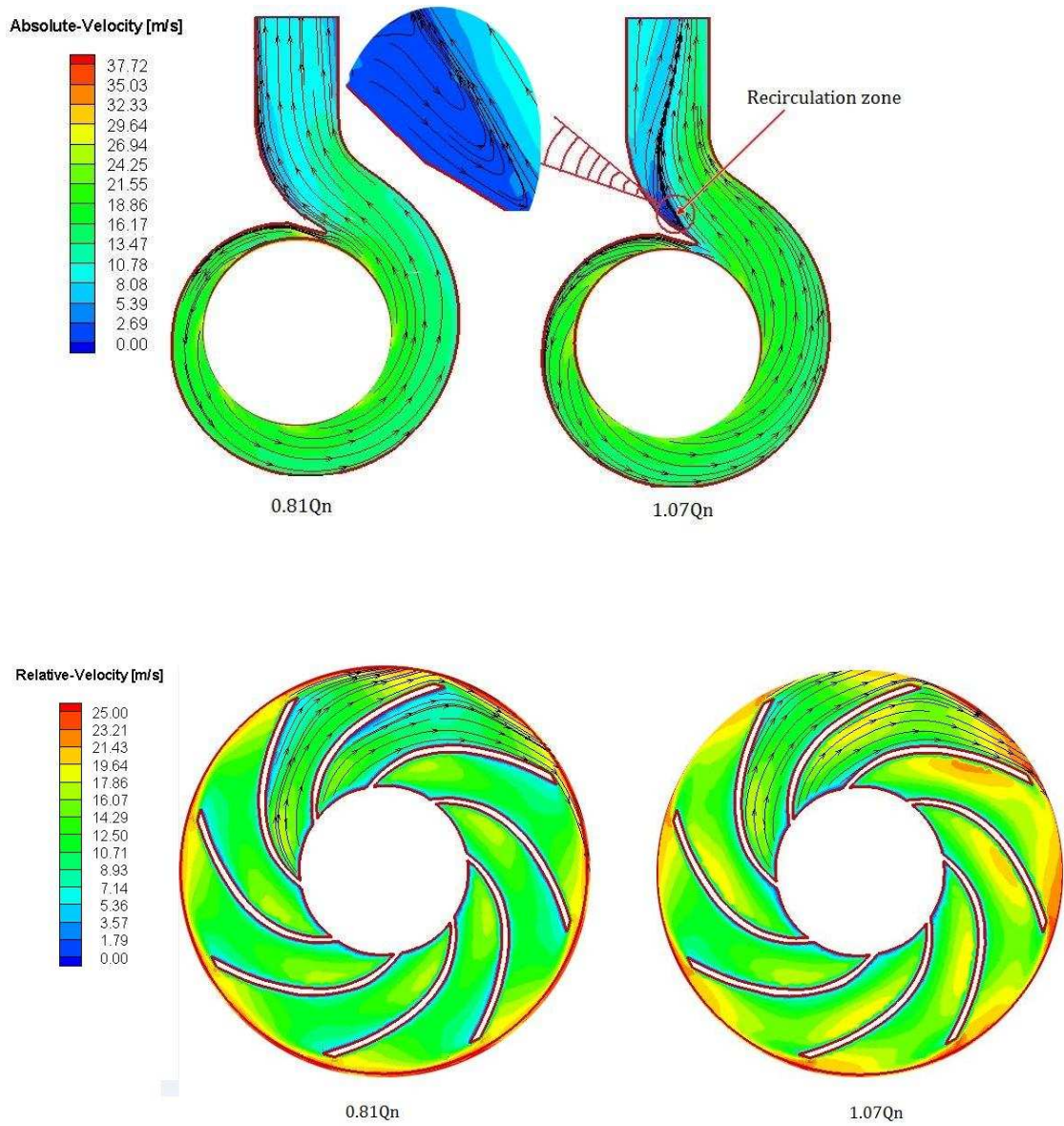


Figure 4: Changes in the flow structure due to off-design conditions, here $Q_n \cong 122$ l/s for this pump. The results were obtained for a section at mid rotor height.



a)

b)

Figure 5: Streamlines inside the pump for a section at mid rotor height: a) flow in the volute casing with a detailed view of a recirculating bubble. b) Flow in the rotor with the velocities represented in the relative frame of reference.

3.2 Running the pump as turbine

Centrifugal pumps have been proposed in the literature to operate in reverse mode¹¹. The operating characteristics were usually obtained with empirical correlations or through experimental testing. By running our numerical model in these operating conditions we can use it as a computational laboratory to study the performance of pumps operating as turbines.

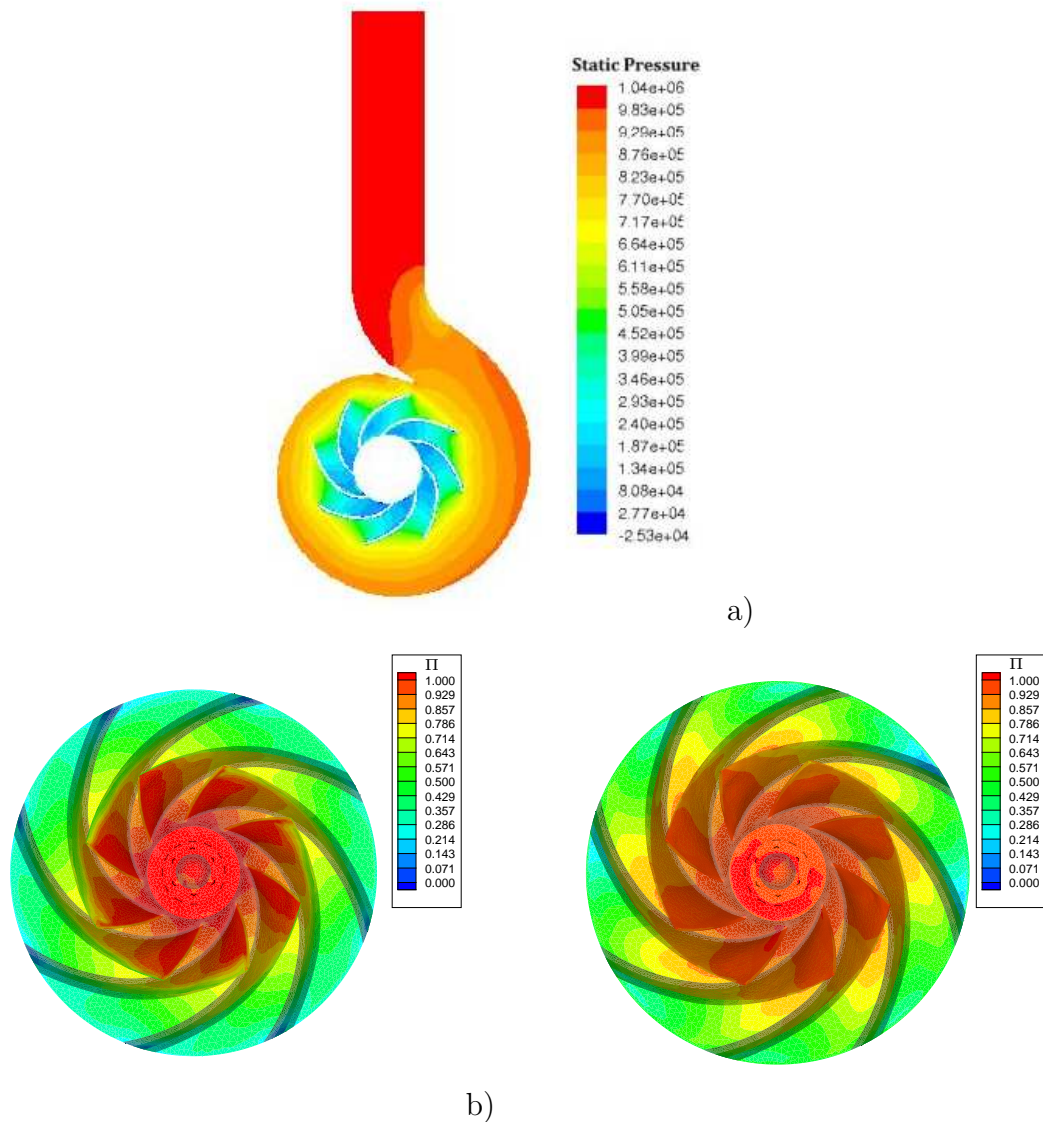


Figure 6: Results obtained for the pump-as-turbine: a) static pressure distribution in turbine mode for a section at mid rotor height. b) Stagnation pressure loss when operating in pump mode at nominal conditions. c) Stagnation pressure loss when operating in pump-as-turbine for the turbine nominal conditions. Values are normalized by rotor inlet stagnation pressure $\Pi = 1 - \frac{P_{tot}}{P_{tot.in}}$.

Some preliminary results were obtained by extrapolating the nominal design point, as a pump, to the nominal design point as a turbine, see Fig.6. Applying Williams correlations we obtained the pressure ratio between inlet (pressure side in pump mode) and outlet (suction side in pump mode). This algebraic correlations can be applied to predict the operating conditions in turbine mode by introducing the maximum efficiency of the pump (in the present computations we have assumed $\eta_{max} = 77\%$);

$$Q_t = \frac{Q_{BEP}}{\eta_{max}^{0.8}} = 151.61l/s,$$

$$H_t = \frac{H_{BEP}}{\eta_{max}^{1.2}} = 112.2meters.$$

We are only required to change static pressure ratio and rotating direction for the pump to me modeled as turbine. The results obtained using our CFD model for turbine mode of operation were $Q = 145.5l/s$ and $H = 113.8$ m (1 116 960.2 Pa). It is interesting to note that operation in pump mode results in quite different pattern of losses, as can be seen in Fig.6-b) and -c).

4 CONCLUSIONS

The paper describes an attempt to model an industrial centrifugal pump as a benchmark test case. One of the main targets achieved was to obtain a computation using a second order spatial discretization for such an intricate geometry as the one presented by this centrifugal pump.

The numerical grid was careful prepared in order to mimic the real geometry. Numerical results were compared with the experiments and the discrepancies are within the expected for a frozen rotor computation. For two off-design working conditions we provide a detailed view of the changes in flow structure, both in terms of pressure distribution and streamline pattern. A detailed description of stagnation pressure losses was presented for the rotor walls. Finally, we have presented results for the operation of the pump in reverse mode. The operation of pump as turbine allows one to obtain a working turbine, for diverse ranges of operation, at a fraction of the economic cost of designing a turbine from scratch.

Acknowledgements

The present work was partial supported by FCT-Research Unit No. 151.

REFERENCES

- [1] Efaflu, Industry - Serie NNJ/NNJM/E-NM - Normalized Pumps, *Efaflu-Bombas e Ventiladores S.A.* (2009).
- [2] D. Croba, J. L. Kueny, Numerical calculation of 2D, unsteady flow in centrifugal pumps: impeller and volute interaction, *International Journal for Numerical Methods in Fluids*, **22** 467–481 (1996).

- [3] J. C. Páscoa, A. C. Mendes, L. M. C. Gato, R. Elder, Aerodynamic design of turbomachinery cascades using an enhanced time-marching finite volume method, *Journal of Computer Modeling in Engineering & Sciences*, **6**(6) 537–546 (2004).
- [4] J. C. Páscoa, A. C. Mendes, L. M. C. Gato, A fast iterative inverse method for turbomachinery blade design, *Mechanics Research Communications*, **36**(5) 537–546 (2009).
- [5] R. A. Van den Braembussche, Flow and loss mechanisms in volutes of centrifugal pumps, *Design and Analysis of High Speed Pumps*, RTO-EN-AVT-143, France, Paper 12 12.1–12.26 (2006).
- [6] S. Kaewnai, M. Chamaoot, S. Wongwises, Predicting performance of radial flow type impeller of centrifugal pump using CFD, *Journal of Mechanical Science and Technology*, **23** 1620–1627 (2009).
- [7] T. W. Ha, A. S. Lee, A modeling of pump impeller shroud and wear-ring seal as a whole, and its application to the pump rotordynamics, *Journal of Mechanical Science and Technology*, **12**(3) 441–450 (1998).
- [8] M. Tan, S. Yuan, H. Liu, Y. Wang, K. Wang, Numerical Research on Performance Prediction for Centrifugal Pumps, *Chinese Journal of Mechanical Engineering*, textbf23(1) 1–6 (2010).
- [9] J. González, J. Fernández, E. Blanco, C. Santolaria, Numerical simulation of the dynamic effects due to impeller-volute interaction in a centrifugal pump, *Journal of Fluids Engineering*, **124** 348–355 (2002).
- [10] R. Spence, J. Amaral-Teixeira, A CFD parametric study of geometrical variations on the pressure pulsations and performance characteristics of a centrifugal pump, *Computers & Fluids*, **38**, 1243-1257 (2009).
- [11] S. Derakhshan, A. Nourbakhsh, Theoretical, numerical and experimental investigation of centrifugal pumps in reverse operation, *Experimental Thermal and Fluid Science*, **32** 1620–1627 (2008).